Cancer Immunol Immunother (2017) 66:1131–1142
DOI 10.1007/s00262-017-2002-2

ORIGINAL ARTICLE

Downregulation of neuropilin-1 on macrophages modulates antibody-mediated tumoricidal activity

Kosuke Kawaguchi[1] · Eiji Suzuki[1] · Mariko Nishie[1] · Isao Kii[2] · Tatsuki R. Kataoka[3] · Masahiro Hirata[3] · Masashi Inoue[1,5] · Fengling Pu[4] · Keiko Iwaisako[4] · Moe Tsuda[1] · Ayane Yamaguchi[1] · Hironori Haga[3] · Masatoshi Hagiwara[2] · Masakazu Toi[1]

Received: 5 October 2016 / Accepted: 16 April 2017 / Published online: 21 April 2017

Abstract Neuropilin-1 (NRP-1)-expressing macrophages are engaged in antitumor immune functions via various mechanisms. In this study, we investigated the role of NRP-1 on macrophages in antibody-mediated tumoricidal activity. Treatment of macrophages with NRP-1 knockdown or an anti-NRP-1-neutralizing antibody significantly suppressed antibody-dependent cellular cytotoxicity and modulated cytokine secretion from macrophages in vitro. Furthermore, in vivo studies using a humanized mouse model bearing human epidermal growth factor receptor-2 (HER2)-positive breast cancer xenografts showed that antibody-mediated antitumor activity and tumor infiltration of $CD4^+$ T lymphocytes were significantly downregulated when peripheral blood mononuclear cells in which NRP-1 was knocked down were co-administered with an anti-HER2 antibody. These results revealed that NRP-1 expressed on macrophages plays an important role in antibody-mediated antitumor immunity. Taken together, the induction of NRP-1 on macrophages may be a therapeutic indicator for antibody treatments that exert antibody-dependent cellular cytotoxicity activity, although further studies are needed in order to support this hypothesis.

Keywords Neuropilin-1 · Breast cancer · HER2 · Humanized mouse · Antibody-dependent cellular cytotoxicity

Abbreviations

ADCC	Antibody-dependent cellular cytotoxicity
EDTA	Ethylenediaminetetraacetic acid
FBS	Fetal bovine serum
GCSF	Granulocyte colony-stimulating factor
Gluc	*Gaussia* luciferase
HER2	Human epidermal growth factor receptor-2
IFN	Interferon
IL	Interleukin
MIP-1α	Macrophage inflammatory protein-1α
MIP-1β	Macrophage inflammatory protein-1β
NOG	Nod/Shi-scid, IL-2Rγ null
NRP-1	Neuropilin-1
PBMCs	Peripheral blood mononuclear cells
PBS	Phosphate-buffered saline
qRT-PCR	Quantitative real-time PCR
RLU	Relative luminescence units
SEM	Standard error of the mean
siRNA	Small interfering RNA
TILs	Tumor-infiltrating lymphocytes
TNF	Tumor necrosis factor
VEGF	Vascular endothelial growth factor

Electronic supplementary material The online version of this article (doi:10.1007/s00262-017-2002-2) contains supplementary material, which is available to authorized users.

✉ Eiji Suzuki
eijis@kuhp.kyoto-u.ac.jp

[1] Department of Breast Surgery, Graduate School of Medicine, Kyoto University, 54 Shogoin-kawaharacho, Sakyo-ku, Kyoto 606-8507, Japan

[2] Department of Anatomy and Developmental Biology, Graduate School of Medicine, Kyoto University, Kyoto, Japan

[3] Department of Diagnostic Pathology, Kyoto University Hospital, Kyoto, Japan

[4] Department of Target Therapy Oncology, Graduate School of Medicine, Kyoto University, Kyoto, Japan

[5] Faculty of Medicine, Gunma University, Gunma, Japan

Introduction

Specific innate and adaptive immune mechanisms are emerging as key modulators of the effects of antibody-mediated tumoricidal activity in various types of cancer [1, 2]. For instance, in breast cancer, innate and acquired immune functions influence the efficacy of antihuman epidermal growth factor receptor-2 (HER2)-targeted antibody therapy in a preclinical model [3, 4]. In the clinical setting, anti-HER2 antibody treatment can remarkably improve the survival outcome of primary breast cancer patients with HER2-positive disease. However, it is also true that the therapeutic effect varies by tumor and by individual [5].

Macrophages are a key subset of immune cells that regulate specific innate and adaptive immune responses [6]. Recent reports have shown that tumor-associated macrophages mediate various immune reactions, such as cytokine secretion, to support and/or inhibit cancer progression, which correlates with prognosis [7–9]. Neuropilin-1 (NRP-1) was initially characterized as a molecule that guides migrating cells and axons in the developing nervous system and is essential for the accurate formation of neurons and vasculature. Several reports have suggested that NRP-1 could be an important molecule for monocyte/macrophage regulation and relevant immune function in tumor microenvironments and that NRP-1-expressing macrophages might play an important role in antitumor activity in tumor microenvironments. NRP-1-expressing monocytes, defined as $CD11b^{+}$ $Gr1^{-}$, possess antitumoral properties [10]. Tordjman et al. reported that macrophages expressing NRP-1 were required for the initiation of primary T cell activation [11]. Casazza et al. found that the NRP-1 pathway is specifically up-regulated in hypoxic areas, where it entraps NRP-1-expressing macrophages, resulting in the accumulation of protumoral macrophages that drive tumor progression [9]. Ji et al. reported that NRP-1 expression is higher in M2 macrophages than in M1 macrophages [12]. Thus, the role of NRP-1 expression on macrophages in immune modulation in tumor microenvironments remains unclear.

To clarify the role of NRP-1 expression on macrophages in antibody-mediated antitumor immunity, here we investigated the impact of NRP-1 knockdown on macrophages and of anti-NRP-1 antibody treatment on antibody-dependent cellular cytotoxicity (ADCC) activity in vitro and also studied its impact on the antitumor immune response in a humanized mouse model of HER2-positive breast cancer.

Materials and methods

Cell lines

SKBR3 cells (HER2-overexpressing human breast cancer cell line) were obtained directly from the American Type Culture Collection (ATCC, Manassas, VA) on September 27, 2013 and passaged in our laboratory for fewer than 6 months after resuscitation. BT474 cells (HER2-overexpressing human breast cancer cell line, HTB-20) were also obtained directly from the ATCC on November 5, 2008 and passaged in our laboratory for fewer than 6 months after resuscitation. BT474 cells were cultured in DMEM containing 10% fetal bovine serum (FBS), and SKBR3 cells were cultured in RPMI 1640 medium containing 10% FBS.

To establish *Gaussia* luciferase (Gluc)-expressing BT474 cells ($BT474^{Gluc}$), BT474 cells were transfected with a Gluc expression vector using polyethylenimine "MAX" (Polysciences, Warrington, PA) and selected using puromycin (Nacalai Tesque, Kyoto, Japan) to establish stable cell lines. The expression vector was constructed by cloning the Gluc coding region into the pCAGIPuro vector (kindly provided by Dr. H. Niwa, RIKEN). pCAGIPuro, an IRES-based bicistronic expression vector in which the gene of interest and a puromycin-resistant gene are expressed from a single mRNA, enables almost all puromycin-selected cells to express the gene product.

Preparation of PBMCs, monocytes, and macrophages

Peripheral blood mononuclear cells (PBMCs) from healthy volunteers were prepared using Vacutainer CPT Cell Preparation Tubes (BD Biosciences, Bedford, MA). Human peripheral blood monocytes were separated from peripheral blood using RosetteSep Human Monocyte Enrichment Cocktail (STEMCELL Technologies, Vancouver, Canada) and magnetic-activated cell sorting with a Monocyte Isolation Kit II (Miltenyi Biotec, Bergisch-Gladbach, Germany), according to the manufacturers' instructions. Although prior reports have shown that macrophage colony-stimulating factor is necessary for NRP-1 expression on dendritic cells and monocyte-derived macrophages [11–13], our optimization experiments showed that it was not always required for an increase in NRP-1 expression on monocyte-derived macrophages (data not shown). In this study, human monocyte-derived macrophages were prepared from adherent monocytes after culture of PBMCs for 24 h in 24-well plates containing RPMI 1640 medium with 10% FBS, and macrophage-depleted PBMCs were prepared by retrieving the floating cells in those culture conditions.

Knockdown of NRP-1 on immune cells by siRNA

Control small interfering RNA (siRNA; Silencer Select Negative Control #1) and siRNA targeting NRP-1 (NRP-1 siRNA s16844 1: sense, 5′-GGUAUGGUGUCUGGACUUATT-3′; antisense, 5′-UAAGUCCAGACACCAUACCCA-3′) (Applied Biosystems, Foster City, CA) were

transfected into PBMCs or macrophages using Lipofectamine RNAiMAX (Life Technologies, Gaithersburg, MD) according to the manufacturer's protocols.

ADCC measurement

ADCC was measured using an LDH Cytotoxic Test Kit (Wako, Osaka, Japan), which has a sensitivity similar to that of the traditional Cr^{51} assay [14]. In the ADCC assay, NRP-1-knocked down macrophages ($Macrophages^{siNRP\text{-}1}$), control macrophages ($Macrophages^{siNC}$), monocytes, and PBMCs were used as effector cells, while SKBR3 cells were used as target cells. Trastuzumab or pertuzumab (Chugai Pharmaceutical Co., Tokyo, Japan) was used as the treatment antibody. The target-to-effector ratio was fixed at 10:1, and the incubation time was set at 24 h based on our optimization experiments (data not shown). ADCC activity was calculated according to the manufacturer's instructions. Cytotoxicity was calculated as % specific lysis = [(effector release − target release) − effector control release] − negative control/(positive control release − negative control release)] × 100. A human NRP-1 monoclonal antibody (AF3870; R&D Systems, Minneapolis, MN) was used to neutralize NRP-1, and IgG (R&D Systems) was used as a control antibody in the ADCC assay.

Humanized mouse model of HER2-positive breast cancer

Female NOD/Shi-scid, IL-2Rγ null (NOG) mice were obtained from the Central Institute for Experimental Animals (Kawasaki, Japan) and used at 6 weeks of age. In vivo experiments were conducted in accordance with the United Kingdom Coordinating Committee on Cancer Research and Guidelines for the Welfare of Animals in Experimental Neoplasia (second edition).

The tumor-bearing NOG mouse model was created using $BT474^{Gluc}$ cells as follows. Briefly, $BT474^{Gluc}$ cells (5.0×10^6) suspended in 80 μL DMEM with 50% Matrigel (BD Biosciences) were injected into the fat pads of 25 NOG mice. The tumor-bearing mice were divided into 5 treatment groups of 5 animals each such that the mean relative luminescence units (RLU) and body weight were equal in each group. The following treatments were given: (i) control (saline), (ii) PBMCs only, (iii) trastuzumab only, (iv) control PBMCs ($PBMC^{siNC}$) + trastuzumab, and (v) NRP-1-knocked down PBMCs ($PBMC^{siNRP\text{-}1}$) + trastuzumab. Tail vein injections of PBMCs (5.0×10^6 cells/mouse) were initiated at 14 days after tumor inoculation when the mean RLU reached 35,072 [±5921, standard error of the mean (SEM)]. Blood samples (5–30 μL) were collected from the tail vein on days 14, 21, and 28.

Tumor specimens were harvested on day 28, and one half of the tumor sample was preserved by formalin fixation, and the other half was immediately placed in liquid nitrogen for RNA and protein extraction.

For the model of NRP-1 knockdown on macrophages, 30 tumor-bearing mice were divided into five treatment groups of six animals each such that the mean RLU were equal in each group. The following treatments were given: (i) control (saline), (ii) PBMCs only, (iii) trastuzumab only, (iv) $Macrophages^{siNRP\text{-}1}$ + PBMCs (macrophages depleted) + trastuzumab, and (v) $Macrophages^{siNC}$ + PBMCs (macrophages depleted) + trastuzumab, and were initiated at 19 days after tumor inoculation. The number of $Macrophages^{siNRP\text{-}1}$ or $Macrophages^{siNC}$ replaced with depleted macrophages was calculated according to the number of macrophages in PBMCs. Blood samples were collected from the tail vein on days 14, 21, 23, 26, 28, and 30. PBMCs injected intravenously and trastuzumab injected intraperitoneally.

Tumor volume monitoring

The greatest longitudinal diameter (length) and greatest transverse diameter (width) were measured with a caliper. Tumor volume was calculated using the ellipsoidal formula as follows: tumor volume = 1/2(length × width^2). We also assessed viable tumor cells by measuring the activity of secreted Gluc in the blood. Measurement of blood Gluc was performed as described previously [15–17]. Briefly, blood samples were diluted with phosphate-buffered saline (PBS) containing 0.02% Tween 20 and 20 mM ethylenediaminetetraacetic acid (EDTA) and stored at −80 °C until use. The luminescence of the diluted blood samples (0.02% Tween 20/20 mM EDTA/PBS buffer) was determined using a Centro LB 960 microplate luminometer (Berthold Technologies, Bad Wildbad, Germany). A reaction mixture containing coelenterazine (final concentration 1 μg/100 μL) in PBS plus 0.02% Tween 20 and 20 mM EDTA was injected into the wells of a plate that was placed into the instrument, and luminescence intensity was recorded at 0.1-s intervals for 10 s or 10 min. Data are expressed as maximum luminescence intensity (I_{max}) in RLU, and the change in RLU was calculated as follows:

RLU % change = [(RLU on day 21 or 28 − RLU on day 14)/RLU on day 14] × 100

RNA extraction and qRT-PCR

Quantitative real-time PCR (qRT-PCR) was performed with TaqMan Fast Virus 1-step Master Mix (Life Technologies) and TaqMan gene expression probes for NRP-1 (Assay ID: Hs00826128_m1), CD4 (Assay ID: Hs01058407_m1),

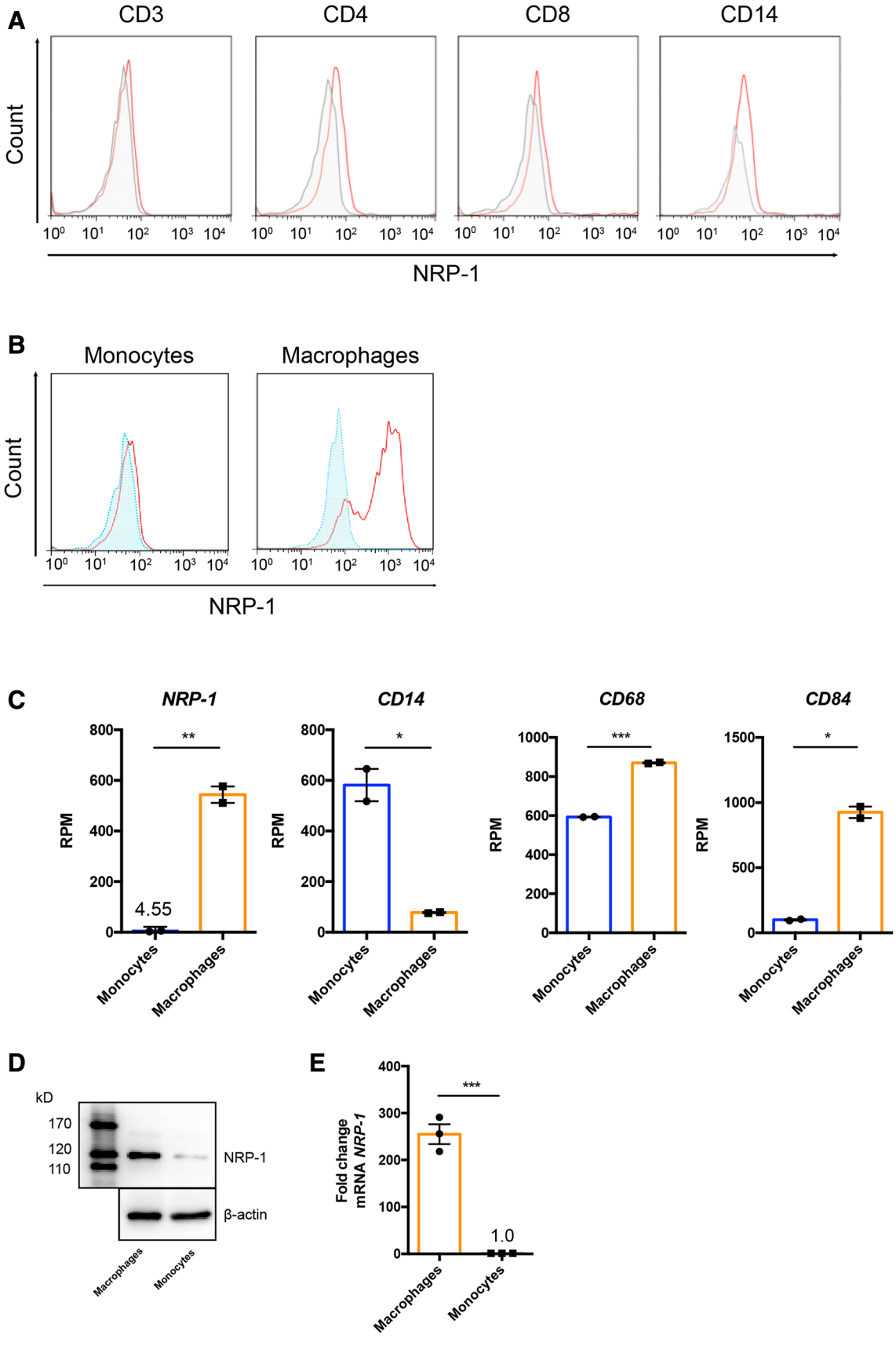
A
CD3
CD4
CD8
CD14
Count
NRP-1
B
Monocytes
Macrophages
Count
NRP-1
C
NRP-1
CD14
CD68
CD84
RPM
4.55
Monocytes
Macrophages
D
kD
170
120
110
NRP-1
β-actin
Macrophages
Monocytes
E
Fold change mRNA NRP-1
1.0
Macrophages
Monocytes

◂**Fig. 1** NRP-1 expression on monocytes and macrophages. **a** NRP-1 expression on $CD3^+$, $CD4^+$, $CD8^+$, and $CD14^+$ cells in fresh PBMCs by flow cytometry. *Gray* isotype control. **b** NRP-1 expression on monocytes (*left*) and macrophages (*right*) by flow cytometry. *Blue* isotype control. **c** NRP-1, CD14, CD68, and CD84 expression on monocytes (*left*) and macrophages (*right*) by RNA sequencing. *RPM* reads per million. $N = 2$. $^*p < 0.05$, $^{**}p < 0.01$, $^{***}p < 0.001$. All *graphs* show mean ± SEM. **d** Protein extracts from monocytes (*right*) and macrophages (*left*). NRP-1 expression was analyzed by western blotting. **e** NRP-1 transcript levels in monocytes (*right*) and macrophages (*left*) by RT-PCR. $N = 3$. $^{***}p < 0.001$. All *graphs* show mean ± SEM

CD8 (Assay ID: Hs00233520_m1), and CD45 (Assay ID: Hs04189704_m1) (Life Technologies).

RNA sequencing

Platelet RNA-Seq analysis was performed on an Ion Proton System for next-generation sequencing (Life Technologies). For each of the samples, 10 ng total RNA was reverse transcribed using an Ion AmpliSeq Transcriptome Human Gene Expression Kit (Life Technologies) following the manufacturer's protocol.

Flow cytometry

PBMCs from healthy volunteers were stained with fluorescein isothiocyanate-conjugated antihuman CD3 (clone UCHT1; Abnova, Taipei, Taiwan), anti-CD4 (clone RPA-T4; BioLegend, San Diego, CA), anti-CD14 (clone 61D3; eBioscience, San Diego, CA), and allophycocyanin-conjugated anti-NRP-1 allophycocyanin monoclonal antibodies (clone 446921, R&D Systems).

Cytokine measurements

The cytokines interleukin (IL)-1β, IL-1γα, IL-2, IL-4, IL-5, IL-6, IL-7, IL-8, IL-9, IL-10, IL-12 (p70), IL-13, IL-15, IL-17, granulocyte–macrophage colony-stimulating factor, granulocyte colony-stimulating factor (GCSF), interferon-gamma (IFN-γ), monocyte chemoattractant protein-1, macrophage inflammatory protein-1α (MIP-1α), macrophage inflammatory protein-1β (MIP-1β), platelet-derived growth factor-BB, RANTES, vascular endothelial growth factor (VEGF), fibroblast growth factor, and tumor necrosis factor α (TNF-α) from the supernatants of macrophages incubated for 24 h were measured on a Bio-Plex multiplex assay system (Bio-Rad, Hercules, CA) according to the manufacturer's instructions. Lysates of whole tumor samples were also prepared using a Bio-Plex lysis kit (Bio-Rad) according to the manufacturer's instructions, and the levels of various cytokines in the tumor lysates were measured on a Bio-Plex multiplex assay system.

Immunohistochemistry

The primary antibodies used for immunohistochemistry and immunofluorescence are listed in Supplemental Table S1. For immunohistochemistry, the sections were incubated with MACH 2 Double Stain 2 (Biocare Medical, Walnut, CA), EnVision HRP (K4001; Dako, Burlingame, CA), or Simple Stain AP (414251; Nichirei Bioscience, Tokyo, Japan) for 1 h.

Evaluation of TILs

Histopathologic assessment of the percentage of tumor-infiltrating lymphocytes (TILs) was performed on one representative immunohistochemical section of a tumor using methods recommended by the International TILs Working Group 2014 [18]. % TILs was defined as the percentage of lymphocyte area per tumor area in vivo samples. Areas of in situ carcinomas, normal lobules, necrosis, hyalinization, and crush artifacts were not included. Histopathologic evaluation of TILs was performed by two breast pathologists who scored each case independently in a blind manner. The mean values of both observers were obtained as the final scores for each case.

Human samples

All samples from healthy volunteers were collected in the Department of Breast Surgery, Kyoto University Hospital. Written informed consent was obtained from all participants prior to sample collection. All study protocols were approved by the Ethics Committee for Clinical Research, Kyoto University Hospital (authorization number G424).

Statistical analysis

The significance of differences between groups was determined by an unpaired two-tailed Student's *t* test or Mann–Whitney test. Results were considered statistically significant at $p < 0.05$. Data were analyzed with STATA version 13.0.

Results

NRP-1 expression on monocytes and macrophages

Previous investigations suggested that NRP-1 is expressed mainly on dendritic cells and monocyte-derived macrophages, but not on monocytes [11, 12]. We used flow cytometry to identify NRP-1-expressing immune cells in samples obtained from healthy volunteers. NRP-1 was expressed primarily on macrophages, but its expression was minor in $CD3^+$, $CD4^+$, $CD8^+$, and $CD14^+$ cells,

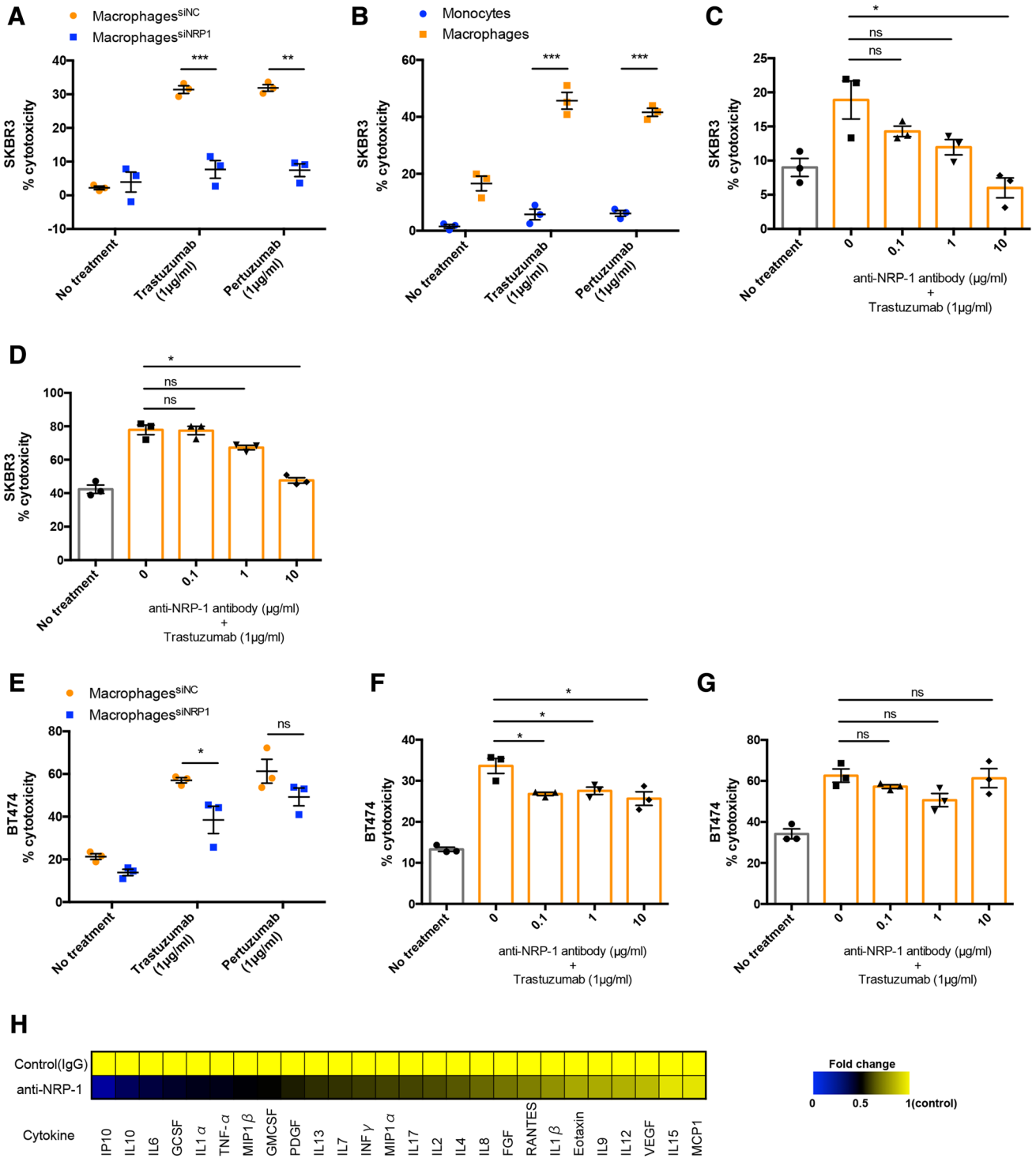

respectively (Fig. 1a, b). Next, we examined the genetic characteristics of monocytes and macrophages using RNA sequencing (GEO accession: GSE75428). *NRP-1* was included in the top 100 up-regulated genes in macrophages as compared with monocytes (Fig. 1c and Supplemental Table S2). In macrophages, CD14, a monocyte marker that is downregulated during monocyte–macrophage differentiation was downregulated compared with monocytes. Conversely, CD68 and CD84, which are representative markers of macrophages, were up-regulated in macrophages (Fig. 1c). Up-regulation of NRP-1 expression on macrophages was also confirmed by qRT-PCR and western blotting (Fig. 1d, e).

◂**Fig. 2** ADCC activity and cytokine secretion are suppressed by NRP-1 inhibition in vitro. A–G. Target cell cytotoxicity was measured by the LDH assay. **a** Macrophages$^{siNRP\text{-}1}$ and Macrophages^{siNC} were co-cultured with target SKBR3 cells and trastuzumab or pertuzumab. **b** Monocytes and macrophages were co-cultured with target SKBR3 cells and trastuzumab or pertuzumab. **c** Macrophages were co-cultured with target SKBR3 cells and trastuzumab with anti-NRP-1 antibodies (0, 0.1, 1, and 10 μg/mL). **d** PBMCs were co-cultured with target SKBR3 cells and trastuzumab with anti-NRP-1 antibodies (0, 0.1, 1, and 10 μg/mL). **e** Macrophages$^{siNRP\text{-}1}$ and Macrophages^{siNC} were co-cultured with target BT474 cells and trastuzumab or pertuzumab. **f** Macrophages were co-cultured with target BT474 cells and trastuzumab with anti-NRP-1 antibodies (0, 0.1, 1, and 10 μg/mL). **g** PBMCs were co-cultured with target BT474 cells and trastuzumab with anti-NRP-1 antibodies (0, 0.1, 1, and 10 μg/mL). The concentration of trastuzumab and pertuzumab was 1 μg/mL, and the effector-to-target ratio was 10:1. $N = 3$ for all experiments. $*p < 0.05$, $**p < 0.01$, $***p < 0.001$, $****p < 0.0001$, *ns* not significant. All *graphs* show mean ± SEM. **h** The effect of the NRP-1-neutralizing antibody on the secretion of 27 cytokines was evaluated and shown by heat map display. Fold change of cytokine expression following NRP-1 inhibition compared to the control group is shown by *yellow-to-blue* color graduation. (Raw data are shown in Table S1.)

ADCC activity and cytokine secretion are suppressed by NRP-1 inhibition in vitro

We investigated the role of NRP-1 expression on macrophages with respect to ADCC, which is one of the major mechanisms of antibody-mediated tumoricidal activity [19]. In this study, we used Macrophages$^{siNRP\text{-}1}$ and Macrophages^{siNC} as effector cells. As the mRNA levels of NRP-1 were raised immediately after seeding on cell culture dishes (Supplemental Figure S2a), NRP-1 knockdown was performed by siRNA administration to fresh monocytes or fresh PBMCs. The average knockdown efficiency was ~65% after 24 h, suggesting that the siRNA used could strongly inhibit NRP-1 expression on monocytes (Supplemental Figure S2b, c). The LDH assay showed that Macrophages$^{siNRP\text{-}1}$ suppressed ADCC activity significantly as compared with Macrophages^{siNC} in both SKBR3 and BT474 cells (Fig. 2a, e), and ADCC activity mediated by macrophages was higher than ADCC activity mediated by monocytes in SKBR3 cells (Fig. 2b). Macrophage-induced ADCC activity was also suppressed by the NRP-1-neutralizing antibody in both SKBR3 and BT474 cells (Fig. 2c, f). PBMC-induced ADCC activity was also suppressed by the NRP-1-neutralizing antibody in SKBR3 cells, but not in BT474 cells (Fig. 2d, g).

Several cytokines augment ADCC by direct activation of immune cells or by enhancement of tumor-associated antigens on tumor cells [20]. Therefore, we tested chemokine secretion in the presence of the NRP-1-neutralizing antibody. The secretion of cytokines by NRP-1-expressing macrophages was suppressed by the NRP-1-neutralizing antibody in vitro (Fig. 2h and raw data in Supplemental Table S3). Additionally, VEGF165, which is a ligand of NRP-1, enhanced the secretion of proinflammatory cytokines from macrophages, such as IP-10, TNF-α, IFN-γ, IL-12, and GCSF. Interestingly, this secretion was suppressed by the NRP-1-neutralizing antibody, while protumoral cytokines, such as IL-1α and IL-10, were not suppressed by treatment with the NRP-1-neutralizing antibody (Supplemental Figure S1).

Knockdown of NRP-1 on PBMCs suppresses anti-HER2 antibody-mediated tumoricidal activity in a humanized mouse model

We further investigated the role of NRP-1 in ADCC in a humanized mouse model with HER2-positive tumors. For this experiment, we used an established humanized mouse model, namely NOG mice [21, 22]. Tumor volume was estimated by measuring the luminescence intensity of peripheral blood from humanized NOG mice transplanted with cancer cells expressing secreted luciferase [17]. We generated luciferase-secreting breast cancer cells by transfection with an expression vector encoding the secreted luminescent protein of *Gaussia princeps*. As BT474 cells show better tumorigenicity than SKBR3 cells, we used BT474 cells in the mouse model. BT474^{Gluc} cells were inoculated into the fat pads of NOG mice, and peripheral blood taken from the tail vein was analyzed for luminescence. Luminescence intensity correlated well with the number of transplanted cells, with a linear range covering over seven orders of magnitude (Supplemental Figure S4a). NRP-1 on PBMCs was knocked down by siNRP-1 before injection via the tail vein. Knockdown efficiency was approximately 65%, and almost all knocked-down cells were macrophages (Supplemental Figure S2b–e). The treatment schema is shown in Supplemental Figure S4b. Relative luminescence between day 21 or 28 and day 14 was evaluated. On day 28, the trastuzumab plus PBMC^{siNC} treatment group showed remarkable inhibition of tumor growth; however, the trastuzumab plus PBMC$^{siNRP\text{-}1}$ group showed only a limited effect that was similar to the trastuzumab alone group, indicating that NRP-1 expression on PBMCs is closely involved with the enhancement of ADCC activity (median: −36.3 vs. 56.3%, $p = 0.035$, Mann–Whitney test) (Fig. 3a–d).

To clarify the role of NRP-1-expressing macrophages more precisely, we replaced the macrophages in PBMCs with NRP-1-knocked down macrophages (adding Macrophages$^{siNRP\text{-}1}$ or Macrophages^{siNC} into macrophage-depleted PBMCs) and tested the efficacy of such PBMCs in the mouse model described above (Fig. 3e, f). The antitumor effect of trastuzumab plus PBMCs with Macrophages$^{siNRP\text{-}1}$ was significantly reduced as

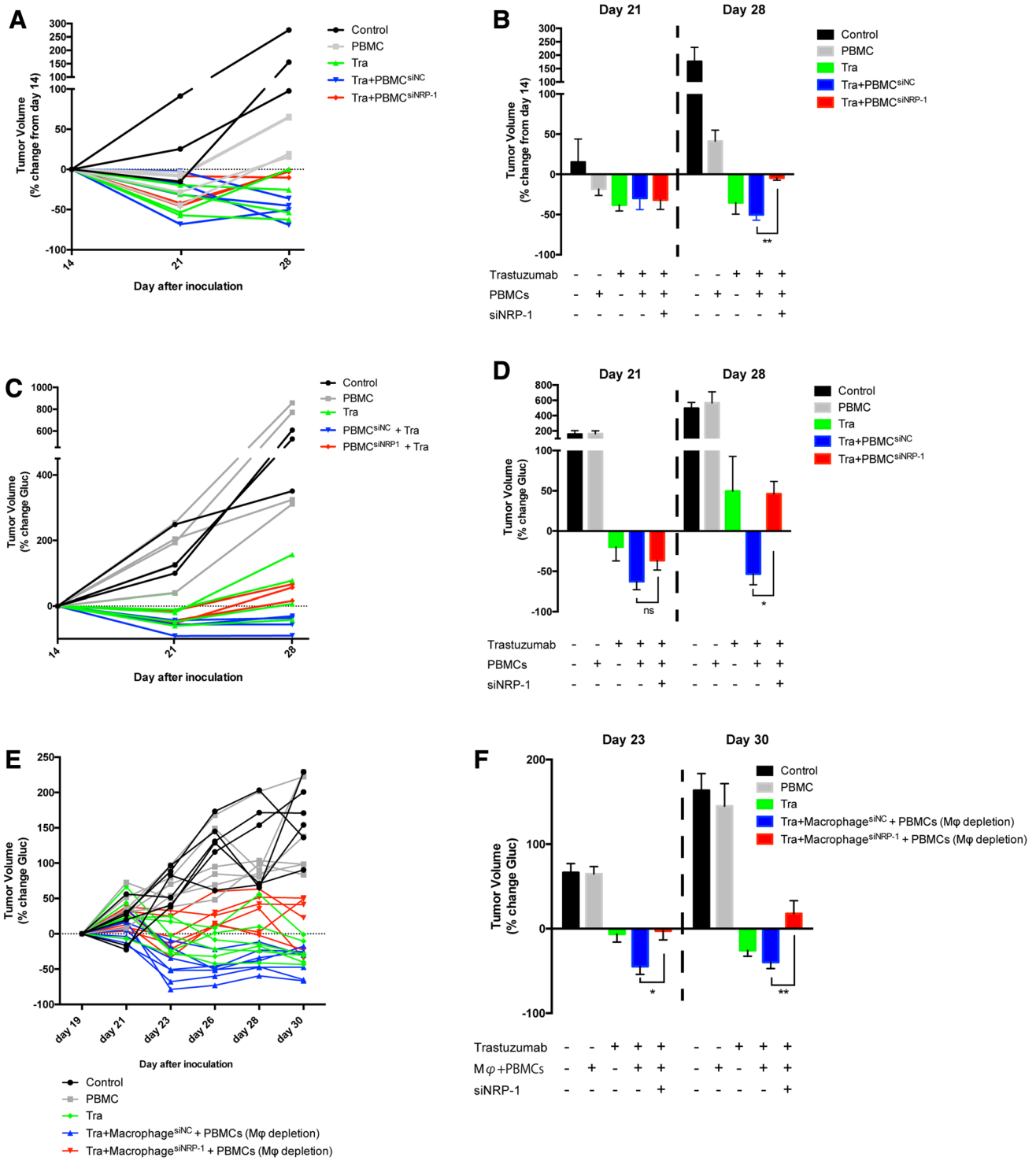

compared with that of trastuzumab plus PBMCs with Macrophages^{siNC} (mean: −39.6% vs. 17.7%, $p = 0.0048$, Mann–Whitney test), further supporting the hypothesis that NRP-1-expressing macrophages play an important role in anti-HER2 antibody-mediated antitumor activity by cooperating with other subsets of immune cells.

Knockdown of NRP-1 on macrophages suppresses lymphocyte infiltration into tumors

Recent reports have shown that anti-HER2 antibody-mediated tumoricidal activity is associated with TILs in breast cancer [18, 23]. We investigated the interaction

◂**Fig. 3** Knockdown of NRP-1 in PBMCs suppresses anti-HER2 antibody-mediated tumoricidal activity in a humanized mouse model. **a**–**d** The tumor-bearing mice were divided into 5 groups of 5 mice each for treatment with (i) control (saline), (ii) human PBMCs, (iii) trastuzumab, (iv) $PBMC^{siNC}$ + trastuzumab, and (v) $PBMC^{siNRP\text{-}1}$ + trastuzumab, such that the mean RLU and body weight were equal in each group. Tail vein injections of trastuzumab (2 μg/g) and/or PBMC (5.0×10^6 cells/mouse) were started at 14 days after tumor inoculation. Blood samples were collected on days 14, 21, and 28. All mice underwent tumorectomy on day 28. **a**, **b** The % change of tumor volume from day 14 to day 19 and to day 28 in each group is shown. **a** Spider plot of each mouse, **b** summary *bar graph* of each group. $N = 3$–5. $^{**}p < 0.01$. All *graphs* show mean ± SEM. **c**, **d** The % change of RLU from day 14 to day 19 and to day 28 in each group is shown. **c** Spider plot of each mouse, **d** summary bar graph of each group. $N = 3$–5. $^{*}p < 0.05$. All graphs show mean ± SEM. E–F. The tumor-bearing mice were divided into 5 groups of 4–6 mice each, and each group was treated with (i) control (saline), (ii) $Macrophages^{siNRP}$ + PBMCs (macrophages depleted) + trastuzumab, and (iii) $Macrophages^{siNC}$ + PBMCs (macrophages depleted) + trastuzumab, such that the mean RLU and body weight were equal in each group. Intraperitoneal injections of trastuzumab (2 μg/g), macrophages (0.5×10^6 cells/mouse), and PBMCs without macrophages (4.5×10^6 cells/mouse) were started at 19 days after tumor inoculation. Blood samples were collected on days 19, 21, 23, 26, 28, and 30. The % change of RLU from day 19. **e** Spider plot of each mouse, **f** summary bar graph of each group. $N = 4$–6. $^{*}p < 0.05$, $^{**}p < 0.01$. All graphs show mean ± SEM

between NRP-1 knockdown and TILs in the humanized mouse model. TILs were identified by immunohistochemical staining and qRT-PCR for CD45, CD4, and CD8, which have no cross-reactivity with mouse immune cells. Injection of human $PBMC^{siNC}$ with trastuzumab yielded much more CD45-positive TILs as compared with the PBMC alone group, and such an increase in TILs was inhibited in the $PBMC^{siNRP\text{-}1}$ group (Fig. 4a). Next, we examined the characteristics of $CD45^+$ TILs by immunohistochemistry (Fig. 4b) and qRT-PCR (Fig. 4c). Most of the $CD45^+$ TILs were positive for CD4 and a small proportion expressed CD8 (Fig. 4c). Lower levels of CD45 transcripts were observed in the $PBMC^{siNRP\text{-}1}$ group compared with the $PBMC^{siNC}$ group (Fig. 4c). Relative quantities of human CD4 mRNA, but not human CD8 mRNA, were also decreased in the $PBMC^{siNRP\text{-}1}$ group (Fig. 4c). We then investigated whether the expression of NRP-1 on macrophages affected the production of various cytokines in vivo. The expression of IP-10, RANTES, MIP-1α, and MIP-1β in tumor samples was suppressed in the NRP-1-knocked down group (Fig. 4d). IP-10, RANTES, MIP-1α, and MIP-1β are mainly secreted from M1 macrophages, which may be attributed to the chemoattraction of $CD4^+$ T cells to tumor sites and enhanced antitumor activity. These results suggested that NRP-1-expressing immune cells, especially macrophages, might play an important role in the migration of CD4-positive immune cells into tumors.

Discussion

ADCC is considered one of the main mechanisms of the antibody-mediated antitumor immune response and is mediated by effector cells such as natural killer cells, monocytes, and macrophages [24]. In this study, we confirmed the importance of macrophages in ADCC activity, while monocytes showed little ADCC activity in our assay (Fig. 2a–g). A recent report showed that tumor-derived semaphorin 3A, which is one of the ligands of NRP-1, augmented the production of antitumoral cytokines, such as IP-10, TNF-α, IFN-γ, and IL-12, and restricted the production of protumoral cytokines, such as IL-1α and IL-10, by macrophages [25]. While various mechanisms regulating macrophage function have been reported, this suggested that the NRP-1 signal in macrophages is one of the important signals for the induction of antitumor immune responses. It was also reported that antitumoral cytokines, such as IL-2, IL-12, TNF-α, and IFN-γ, which are representative Th1 cytokines, enhanced ADCC activity [20]. Thus, our findings that inhibition of NRP-1 on macrophages suppressed the secretion of antitumoral cytokines, such as IP-10, TNF-α, and IFN-γ (Fig. 2h), and that the VEGF165-induced secretion of IL-1α, IL-10, IP-10, TNF-α, IFN-γ, and IL-12 was suppressed by the anti-NRP-1 antibody (Supplemental Figure S1), might explain why NRP-1 knockdown on macrophages suppressed ADCC activity in vitro (Fig. 2a, e) and in our mouse model (Fig. 3a–f).

Regulation of M1 and M2 macrophages in the breast cancer microenvironment is important in antitumor immunity. NRP-1 expression is higher in M2 macrophages than in M1 macrophages (Supplemental Figure S3a) [12, 25], suggesting that NRP-1 expression plays an important role in the polarization of M2 macrophages. Conversely, we confirmed that the cytokines secreted mainly by M1 macrophages are suppressed when NRP-1 was inhibited by neutralizing antibodies (Fig. 2h). Wallerius et al. reported that SEMA3A induced the proliferation of M1 macrophages, which resulted in the increased phosphorylation of Akt and MAPK through NRP-1 [25]. Thus, it is suggested that NRP-1 might play an important role in M1 macrophages in terms of their antitumor immunity. Further study will be needed to resolve the roles of NRP-1 in macrophages.

The presence of TILs is associated with better outcomes in patients with various types of cancer who receive adjuvant or neoadjuvant antibody agent-based systemic therapy [23, 26, 27]. The precise analysis of TIL subsets could be important to understand the role of TILs in tumor microenvironments. Our study showed that NRP-1 knockdown suppressed the infiltration

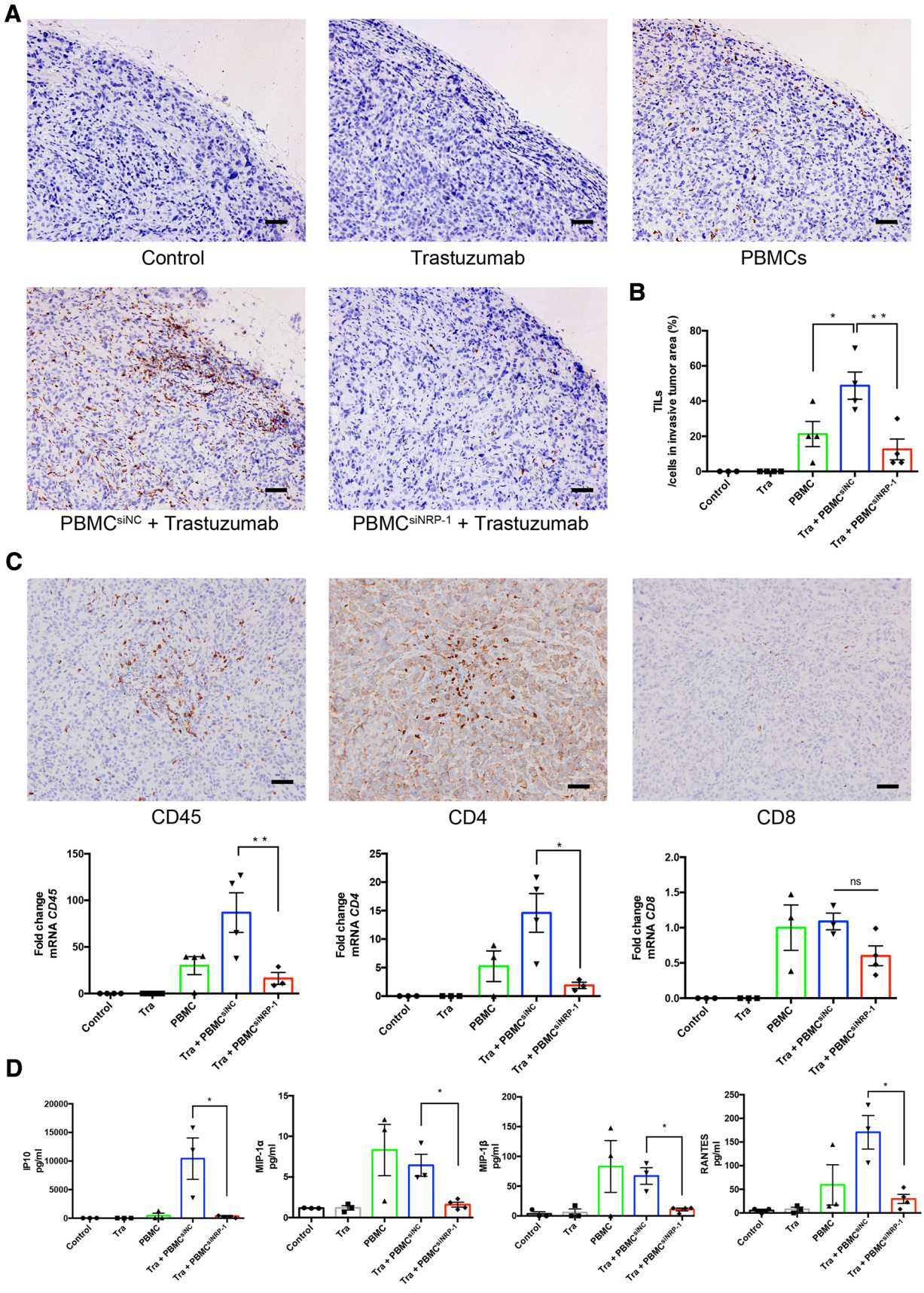
A
Control
Trastuzumab
PBMCs
PBMC^siNC + Trastuzumab
PBMC^siNRP-1 + Trastuzumab
B
TILs /cells in invasive tumor area (%)
Control
Tra
PBMC
Tra + PBMC^siNC
Tra + PBMC^siNRP-1
C
CD45
CD4
CD8
Fold change mRNA CD45
Fold change mRNA CD4
Fold change mRNA CD8
ns
D
IP10 pg/ml
MIP-1α pg/ml
MIP-1β pg/ml
RANTES pg/ml

◂**Fig. 4** Knockdown of NRP-1 on PBMCs suppresses lymphocyte infiltration into tumors. **a** CD45 staining of tumor tissues in each group is shown (*scale bar*, 100 μm). **b** Population of % TILs in five groups. TILs were defined as % CD45-positive cells in the invasive tumor area. $N = 3$–4. $*p < 0.05$, $**p < 0.01$, $***p < 0.001$. All *graphs* show mean ± SEM. **c** *Upper* CD45, CD4, and CD8 staining of tumor tissues in $PBMC^{siNC}$ + Trastuzumab group is shown (*scale bar*, 100 μm). *Lower* CD45, CD4, and CD8 mRNA expression of tumor tissues in each group in day 28 tumors is shown. $N = 3$–4. $*p < 0.05$, $**p < 0.01$, $***p < 0.001$, *ns* not significant. All *graphs* show mean ± SEM. **d** Secretion of IP-10, RANTES, MIP-1α, and MIP-1β from tumor samples was suppressed by NRP-1 knockdown. $N = 3$–4. $*p < 0.05$. All graphs show mean ± SEM

of $CD45^+$ immune cells into tumors in a humanized mouse model (Fig. 4a, b). Importantly, the infiltration of $CD4^+$ cells into tumors was significantly suppressed by NRP-1 knockdown on PBMCs (Fig. 4c). Macrophages are reported to produce chemokines, including IP-10, MIP-1α, MIP-1β, and RANTES, to attract $CD4^+$ T cells [28, 29]. $CD4^+$ T cells exert their anticancer actions by providing help to $CD8^+$ T cells followed by the secretion of type 1 cytokines or direct tumor killing [30–32]. These observations and our findings indicate that NRP-1 on macrophages may regulate $CD4^+$ T cell infiltration into tumors and modulate adaptive immune responses in addition to antibody-mediated innate tumoricidal activity.

We acknowledge that this study has several limitations. In particular, the immune cells used were collected from healthy volunteers and allogenic antitumor immune reactions were not excluded completely. However, because it has been suggested that the functions of NRP-1 are different between human and mouse immune cells, we used the humanized mice model in this study in order to try to elucidate a role for NRP-1 in human macrophages even if allogenic effects could exist. Another limitation would be that an extended time course analysis of the role of NRP-1 in macrophages in this humanized mice model was not conducted. As NRP-1 expression in siNC PBMCs almost disappeared within 96 h due to the difficulty of maintaining the viability of PBMCs in long-term culture without stimulation in vitro, it is difficult to evaluate how long NRP-1 knockdown lasts in macrophages (Supplemental Figure S2f). However, it is known that the knockdown effect of siRNA lasts for approximately 5 days, and NRP-1 expression would be restored thereafter; therefore, NRP-1 in macrophages might mainly function in the acute setting of antitumor activity in vivo. Further research will be needed to elucidate this issue.

In conclusion, we demonstrated that NRP-1 expression on macrophages is required for antibody-mediated tumoricidal activity and $CD4^+$ T cell infiltration into tumor sites by performing in vitro and in vivo experiments with a human breast cancer xenograft model. We propose that regulation of the NRP-1 pathway in macrophages may induce an antitumor immune response by creating a favorable tumor microenvironment, and the presence of tumor-infiltrating NRP-1-expressing immune cells may be beneficial for producing a better response. In addition, NRP-1 expression on macrophages may be a therapeutic indicator for antibody treatments exerting ADCC activity, although further studies are needed to support this hypothesis.

Acknowledgements We thank the medical staff of the Department of Breast Surgery of Kyoto University Hospital for their help in the recruitment of participants and collection of samples. We also thank Dr. Hitoshi Niwa (RIKEN CDB, Kobe, Japan) for providing the pCA-GIPuro vector.

Compliance with ethical standards

Conflict of interest The authors declare no conflicts of interests.

Ethical approval All procedures performed in studies involving human participants were in accordance with the ethical standards of the institutional and/or national research committee and with the 1964 Helsinki declaration and its later amendments or comparable ethical standards. All applicable international, national, and/or institutional guidelines for the care and use of animals were followed. All procedures performed in studies involving animals were in accordance with the ethical standards of the institution or practice at which the studies were conducted.

Financial support This research was supported by a grant from the Japan Society for the Promotion of Science (KAKENHI Grant Number 12907996).

References

1. Bellati F, Napoletano C, Ruscito I, Liberati M, Panici PB, Nuti M (2010) Cellular adaptive immune system plays a crucial role in trastuzumab clinical efficacy. J Clin Oncol 28:e369–e370. doi:10.1200/JCO.2010.28.6922 **(author reply e71)**
2. Ferris RL, Jaffee EM, Ferrone S (2010) Tumor antigen-targeted, monoclonal antibody-based immunotherapy: clinical response, cellular immunity, and immunoescape. J Clin Oncol 28:4390–4399. doi:10.1200/JCO.2009.27.6360
3. Park S, Jiang Z, Mortenson ED et al (2010) The therapeutic effect of anti-HER2/neu antibody depends on both innate and adaptive immunity. Cancer Cell 18:160–170. doi:10.1016/j.ccr.2010.06.014
4. Stagg J, Loi S, Divisekera U, Ngiow SF, Duret H, Yagita H, Teng MW, Smyth MJ (2011) Anti-ErbB-2 mAb therapy requires type I and II interferons and synergizes with anti-PD-1 or anti-CD137 mAb therapy. Proc Natl Acad Sci USA 108:7142–7147. doi:10.1073/pnas.1016569108
5. Piccart-Gebhart MJ, Procter M, Leyland-Jones B et al (2005) Trastuzumab after adjuvant chemotherapy in HER2-positive breast cancer. N Engl J Med 353:1659–1672
6. Pollard JW (2004) Tumour-educated macrophages promote tumour progression and metastasis. Nat Rev Cancer 4:71–78. doi:10.1038/nrc1256
7. Leek RD, Lewis CE, Whitehouse R, Greenall M, Clarke J, Harris AL (1996) Association of macrophage infiltration with

angiogenesis and prognosis in invasive breast carcinoma. Cancer Res 56:4625–4629
8. Gwak JM, Jang MH, Kim DI, Seo AN, Park SY (2015) Prognostic value of tumor-associated macrophages according to histologic locations and hormone receptor status in breast cancer. PLoS One 10:e0125728. doi:10.1371/journal.pone.0125728
9. Casazza A, Laoui D, Wenes M et al (2013) Impeding Macrophage Entry into Hypoxic Tumor Areas by Sema3A/Nrp1 Signaling Blockade Inhibits Angiogenesis and Restores Antitumor Immunity. Cancer Cell 24:695–709. doi:10.1016/j.ccr.2013.11.007
10. Carrer A, Moimas S, Zacchigna S et al (2012) Neuropilin-1 identifies a subset of bone marrow Gr1- monocytes that can induce tumor vessel normalization and inhibit tumor growth. Cancer Res 72:6371–6381. doi:10.1158/0008-5472.CAN-12-0762
11. Tordjman R, Lepelletier Y, Lemarchandel V, Cambot M, Gaulard P, Hermine O, Romeo PH (2002) A neuronal receptor, neuropilin-1, is essential for the initiation of the primary immune response. Nat Immunol 3:477–482. doi:10.1038/ni789
12. Ji JD, Park-Min KH, Ivashkiv LB (2009) Expression and function of semaphorin 3A and its receptors in human monocyte-derived macrophages. Hum Immunol 70:211–217. doi:10.1016/j.humimm.2009.01.026
13. Takamatsu H, Takegahara N, Nakagawa Y et al (2010) Semaphorins guide the entry of dendritic cells into the lymphatics by activating myosin II. Nat Immunol 11:594–600. doi:10.1038/ni.1885
14. Broussas M, Broyer L, Goetsch L (2013) Evaluation of antibody-dependent cell cytotoxicity using lactate dehydrogenase (LDH) measurement. Methods Mol Biol 988:305–317. doi:10.1007/978-1-62703-327-5_19
15. Wurdinger T, Badr C, Pike L, de Kleine R, Weissleder R, Breakefield XO, Tannous BA (2008) A secreted luciferase for ex vivo monitoring of in vivo processes. Nat Methods 5:171–173. doi:10.1038/nmeth.1177
16. Chung E, Yamashita H, Au P, Tannous BA, Fukumura D, Jain RK (2009) Secreted Gaussia luciferase as a biomarker for monitoring tumor progression and treatment response of systemic metastases. PLoS One 4:e8316. doi:10.1371/journal.pone.0008316
17. Tannous BA (2009) Gaussia luciferase reporter assay for monitoring biological processes in culture and in vivo. Nat Protoc 4:582–591. doi:10.1038/nprot.2009.28
18. Salgado R, Denkert C, Demaria S et al (2014) Harmonization of the evaluation of tumor infiltrating lymphocytes (TILs) in breast cancer: recommendations by an international TILs-working group 2014. Ann Oncol. doi:10.1093/annonc/mdu450
19. Valabrega G, Montemurro F, Aglietta M (2007) Trastuzumab: mechanism of action, resistance and future perspectives in HER2-overexpressing breast cancer. Ann Oncol 18:977–984. doi:10.1093/annonc/mdl475
20. Flieger D, Spengler U, Beier I, Kleinschmidt R, Hoff A, Varvenne M, Sauerbruch T, Schmidt-Wolf I (1999) Enhancement of antibody dependent cellular cytotoxicity (ADCC) by combination of cytokines. Hybridoma 18:63–68. doi:10.1089/hyb.1999.18.63
21. Hiramatsu H, Nishikomori R, Heike T, Ito M, Kobayashi K, Katamura K, Nakahata T (2003) Complete reconstitution of human lymphocytes from cord blood CD34$^+$ cells using the NOD/SCID/γcnull mice model. Blood 102:873–880. doi:10.1182/blood-2002-09-2755
22. Ito A, Ishida T, Yano H et al (2009) Defucosylated anti-CCR4 monoclonal antibody exercises potent ADCC-mediated antitumor effect in the novel tumor-bearing humanized NOD/Shi-scid, IL-2Rgamma(null) mouse model. Cancer Immunol Immunother 58:1195–1206. doi:10.1007/s00262-008-0632-0
23. Denkert C, von Minckwitz G, Brase JC et al (2015) Tumor-infiltrating lymphocytes and response to neoadjuvant chemotherapy with or without carboplatin in human epidermal growth factor receptor 2-positive and triple-negative primary breast cancers. J Clin Oncol 33:983–991. doi:10.1200/JCO.2014.58.1967
24. Shaw GM, Levy PC, LoBuglio AF (1978) Human monocyte antibody-dependent cell-mediated cytotoxicity to tumor cells. J Clin Investig 62:1172–1180. doi:10.1172/JCI109236
25. Wallerius M, Wallmann T, Bartish M et al (2016) Guidance molecule SEMA3A restricts tumor growth by differentially regulating the proliferation of tumor-associated macrophages. Cancer Res 76:3166–3178. doi:10.1158/0008-5472.CAN-15-2596
26. Denkert C, Loibl S, Noske A et al (2010) Tumor-associated lymphocytes as an independent predictor of response to neoadjuvant chemotherapy in breast cancer. J Clin Oncol 28:105–113. doi:10.1200/JCO.2009.23.7370
27. Loi S, Michiels S, Salgado R et al (2014) Tumor infiltrating lymphocytes are prognostic in triple negative breast cancer and predictive for trastuzumab benefit in early breast cancer: results from the FinHER trial. Ann Oncol 25:1544–1550. doi:10.1093/annonc/mdu112
28. Dufour JH, Dziejman M, Liu MT, Leung JH, Lane TE, Luster AD (2002) IFN-gamma-inducible protein 10 (IP-10; CXCL10)-deficient mice reveal a role for IP-10 in effector T cell generation and trafficking. J Immunol 168:3195–3204
29. Wu L, Adams M, Carter T, Chen R, Muller G, Stirling D, Schafer P, Bartlett JB (2008) Lenalidomide enhances natural killer cell and monocyte-mediated antibody-dependent cellular cytotoxicity of rituximab-treated CD20$^+$ tumor cells. Clin Cancer Res 14:4650–4657. doi:10.1158/1078-0432.CCR-07-4405
30. Donia M, Hansen M, Sendrup SL, Iversen TZ, Ellebaek E, Andersen MH, Straten P, Svane IM (2013) Methods to improve adoptive T-cell therapy for melanoma: IFN-gamma enhances anticancer responses of cell products for infusion. J Invest Dermatol 133:545–552. doi:10.1038/jid.2012.336
31. Friedman KM, Prieto PA, Devillier LE, Gross CA, Yang JC, Wunderlich JR, Rosenberg SA, Dudley ME (2012) Tumor-specific CD4$^+$ melanoma tumor-infiltrating lymphocytes. J Immunother 35:400–408. doi:10.1097/CJI.0b013e31825898c5
32. Quezada SA, Simpson TR, Peggs KS et al (2010) Tumor-reactive CD4(+) T cells develop cytotoxic activity and eradicate large established melanoma after transfer into lymphopenic hosts. J Exp Med 207:637–650. doi:10.1084/jem.20091918